Biological control of toxic cyanobacteria by mixotrophic predators: an experimental test of intraguild predation theory

Wilken, S.; Verspagen, J.M.H.; Naus-Wiezer, S.M.H.; Van Donk, E.; Huisman, Jef

published in
Ecological Applications
2014

DOI (link to publisher)
10.1890/13-0218.1

document version
Peer reviewed version

ECOLOGICAL SOCIETY OF AMERICA

Ecology/Ecological Monographs/Ecological Applications

PREPRINT

The doi for this manuscript and the correct format for citing the paper are given at the top of the online (html) abstract.

Once the final published version of this paper is posted online, it will replace the preliminary version at the specified doi.

Running head: Biocontrol of harmful cyanobacteria

Biological control of toxic cyanobacteria by mixotrophic predators: an experimental test of intraguild predation theory

Susanne Wilken[1,2,4,5], Jolanda M. H. Verspagen[2], Suzanne Naus-Wiezer[1], Ellen Van Donk[1,3], and Jef Huisman[2]

[1] Department of Aquatic Ecology, Netherlands Institute of Ecology (NIOO-KNAW), Wageningen, The Netherlands

[2] Aquatic Microbiology, Institute for Biodiversity and Ecosystem Dynamics, University of Amsterdam, Amsterdam, The Netherlands

[3] Department of Ecology and Biodiversity, University of Utrecht, Utrecht, The Netherlands

[4] Now at: Monterey Bay Aquarium Research Institute (MBARI), Moss Landing, CA, USA

[5] corresponding author: swilken@mbari.org

Abstract

Intraguild predators both feed on and compete with their intraguild prey. In theory, intraguild predators can therefore be very effective as biological control agents of intraguild prey species, especially in productive environments. We investigated this hypothesis using the mixotrophic chrysophyte *Ochromonas* as intraguild predator and the harmful cyanobacterium *Microcystis aeruginos*a as its prey. *Ochromonas* can grow photoautotrophically, but can also graze efficiently on *Microcystis*. Hence, it competes with its prey for inorganic resources. We developed a mathematical model and parameterized it for our experimental food web. The model predicts dominance of *Microcystis* at low nutrient loads, coexistence of both species at intermediate nutrient loads, and dominance of *Ochromonas* but a strong decrease of *Microcystis* at high nutrient loads. We tested these theoretical predictions in chemostat experiments supplied with three different nitrogen concentrations. *Ochromonas* initially suppressed the *Microcystis* abundance by > 97% compared to the *Microcystis* monocultures. Thereafter, however, *Microcystis* gradually recovered to ~20% of its monoculture abundance at low nitrogen loads, but to 50-60% at high nitrogen loads. Hence, *Ochromonas* largely lost control over the *Microcystis* population at high nitrogen loads. We explored several mechanisms that might explain this deviation from theoretical predictions, and found that intraspecific interference at high *Ochromonas* densities reduced their grazing rates on *Microcystis*. These results illustrate the potential of intraguild predation to control pest species, but also show that the effectiveness of their biological control can be reduced in productive environments.

Keywords: omnivory, mixotrophy, eutrophication, toxic cyanobacteria, predator-prey interactions, resource competition, lake restoration

Introduction

Studies of competition and predation, the two major structuring forces of ecological food webs, have played a key role in the development of community ecology. Intraguild predation encompasses both types of species interaction (Polis et al. 1989, Polis and Holt 1992). Intraguild predation is defined as "the killing and eating of species that use similar resources and are thus potential competitors" (Polis and Holt 1992). In other words, intraguild predators eat their competitors. Attacking prey from two sides, through both competition and predation, can be a very efficient strategy to suppress the population abundances of intraguild prey (Polis and Holt 1992, Thingstad et al. 1996). Therefore, intraguild predators that utilize pest species as their intraguild prey might be very effective as biological control agents (Bampfylde and Lewis 2007).

Most models predict coexistence of intraguild predators and their prey in habitats of intermediate productivity, provided that the intraguild prey is a better competitor for the common resource (Polis and Holt 1992, Holt and Polis 1997, Diehl and Feissel 2000). However, intraguild prey populations are predicted to decrease with increasing productivity due to an enhanced predation pressure, and intraguild predators will tend to exclude their intraguild prey from highly productive environments (Holt and Polis 1997, Diehl and Feissel 2000, Mylius et al. 2001, Van de Wolfshaar et al. 2006). These theoretical predictions are supported to various degrees by microcosm experiments with aquatic protists (Morin 1999, Diehl and Feissel 2000, 2001) and by field experiments with an insect and its parasitoids (Borer et al. 2003). Yet, other experiments observed persistence of intraguild prey in productive environments (Liess and Diehl 2006, Montserrat et al. 2008). Moreover, coexistence of intraguild predators and their prey appears widespread in natural communities, including productive environments (Polis and Strong 1996, Arim and Marquet 2004). During recent years, theoretical studies have therefore proposed a plethora of possible mechanisms that promote the persistence of intraguild prey in productive

environments (e.g., Křivan and Diehl 2005, Finke and Denno 2006, Janssen et al. 2007, Amarasekare 2008, Rudolf and Armstrong 2008, Abrams and Fung 2010, Hin et al. 2011).

Intraguild predation has received considerable interest in agricultural studies (Rosenheim et al. 1995, Straub et al. 2008, Van Maanen et al. 2012), but may also find application in other fields including water management. In particular, cyanobacterial blooms are favored by high nutrient loads, and have increasingly become a major nuisance in many lakes and reservoirs (Chorus and Bartram 1999, Huisman et al. 2005, Paerl and Huisman 2008). Dense cyanobacterial blooms may cause nighttime oxygen depletion, sometimes leading to large fish kills. In addition, the high turbidity of cyanobacterial blooms reduces the growth of aquatic macrophytes, suppressing important underwater habitat for other aquatic organisms (Scheffer 1998). Furthermore, several cyanobacterial species can produce toxins causing serious and sometimes fatal liver, digestive and neurological diseases in birds, mammals (e.g., pets, cattle) and humans (Codd 1995, Carmichael et al. 2001). Cyanobacterial blooms are therefore a major concern in water quality management (Codd et al. 2005, Verspagen et al. 2006, Qin et al. 2010).

Mixotrophic organisms combine autotrophic and heterotrophic nutrition. For instance, many photosynthetic microalgae can also ingest bacteria and phytoplankton species by phagocytosis (Stoecker 1998, Jones 2000). Hence, mixotrophs often act as intraguild predators that compete with phytoplankton species for nutrients and light, but also graze upon them (Thingstad et al. 1996). Mixotrophs are widespread in plankton communities of both freshwater and marine ecosystems (Isaksson 1998, Zubkov and Tarran 2008, Hartmann et al. 2012, Flynn et al. 2013), and several species are capable to form dense blooms in eutrophic environments (Burkholder et al. 2008). In particular, some mixotrophic chrysophytes of the *Ochromonas* genus can graze efficiently on toxic cyanobacteria, and are even capable of degrading cyanobacterial toxins (Van Donk et al. 2009, Wilken et al. 2010). Their function as intraguild predators might

make these mixotrophs ideal candidates as biological control agents against harmful cyanobacteria in eutrophic lakes.

In this paper, we test the predictions of intraguild predation theory with the toxic cyanobacterium *Microcystis aeruginosa* as intraguild prey and the mixotroph *Ochromonas* sp. as intraguild predator. We first develop a simple model to describe the population dynamics generated by intraguild predation along a productivity gradient. The model predictions are tested in a series of chemostat experiments at three different nitrogen levels to create an experimental productivity gradient. The experimental results are used to evaluate the potential for mixotrophic predators to control the development of harmful cyanobacterial blooms in productive environments.

Theory

Model structure

Our model is a variant of the earlier intraguild predation models developed by Holt and Polis (1997) and Diehl and Feissel (2000). These authors assumed that the basal resource was a living organism (e.g., a bacterium) obeying logistic growth, the intraguild prey was a heterotroph feeding on the basal prey, and the intraguild predator consumed both the basal and intraguild prey. In our application, the basal resource is an inorganic nutrient, the intraguild prey is an autotrophic organism that takes up inorganic nutrients from the environment, and the intraguild predator is a mixotroph that obtains nutrients through both uptake of inorganic nutrients and ingestion of the autotrophic prey (Wilken et al. 2013a).

We consider a variable-internal-stores model, where nutrients are first taken up by the organisms, and subsequently the organisms can utilize the stored nutrients for population growth (Droop 1973, Grover 1991). Let N denote the concentration of dissolved inorganic nutrient, let

112 Q_A and Q_M denote the cellular nutrient contents of the autotroph and mixotroph, respectively, and
113 let A and M denote the population densities of the autotroph and mixotroph. Our intraguild
114 predation model then reads:

115 $$\frac{dN}{dt} = D(N_{in} - N) - u_A(N,Q_A)A - u_M(N,Q_M)M \quad (1)$$

116 $$\frac{dQ_A}{dt} = u_A(N,Q_A) - \mu_A(Q_A)Q_A \quad (2)$$

117 $$\frac{dQ_M}{dt} = u_M(N,Q_M) + f_M(A)Q_A - \mu_M(Q_M)Q_M \quad (3)$$

118 $$\frac{dA}{dt} = \mu_A(Q_A)A - f_M(A)M - m_A A \quad (4)$$

119 $$\frac{dM}{dt} = \mu_M(Q_M)M - m_M M \quad (5)$$

120 Here, D is the nutrient turnover rate, N_{in} is the nutrient load, $u_A(N,Q_A)$ and $u_M(N,Q_M)$ are the
121 nutrient uptake rates of the autotroph and mixotroph, $\mu_A(Q_A)$ and $\mu_M(Q_M)$ are the specific growth
122 rates of the autotroph and mixotroph as functions of their cellular nutrient status, $f_M(A)$ is the
123 functional response of the mixotroph grazing upon its autotrophic prey, and m_A and m_M are the
124 mortality rates of the autotroph and mixotroph, respectively.

125 We assume that the nutrient uptake rates of the autotroph and mixotroph increase with the
126 ambient nutrient concentration according to Michaelis-Menten kinetics, and are suppressed when
127 cells become satiated with nutrient (Morel 1987, Ducobu et al. 1998):

128 $$u_i(N,Q_i) = \frac{u_{\max,i}N}{K_i + N}\left(\frac{Q_{\max,i} - Q_i}{Q_{\max,i} - Q_{\min,i}}\right) \qquad i=A,M \quad (6)$$

129 where $u_{max,i}$ is the maximum nutrient uptake rate of species i, K_i is its half-saturation constant for
130 nutrient uptake, and $Q_{\max,i}$ and $Q_{\min,i}$ are its maximum and minimum cellular nutrient contents,
131 respectively.

The model further assumes that the specific growth rates of the autotroph and mixotroph are increasing saturating functions of their cellular nutrient status:

$$\mu_i(Q_i) = \mu_{\max,i}\left(1 - \frac{Q_{\max,i} - Q_i}{Q_{\max,i} - Q_{\min,i}}\right) \qquad i=A,M \qquad (7)$$

where $\mu_{\max,i}$ is the maximum specific growth rate of species i. This formulation resembles Droop's (1973) classic growth equation, but in addition to a minimum cellular nutrient content it also incorporates a maximum cellular nutrient content.

The mixotroph feeds upon the autotroph with a Holling type III functional response, in accordance with the experimental data of Wilken et al. (2010):

$$f_M(A) = \frac{f_{\max}(A/k_M)^b}{1+(A/k_M)^b} \qquad (8)$$

where f_{max} is the maximum ingestion rate, k_M is the half-saturation constant for prey ingestion, and b describes the curvature of the type III functional response.

Our model assumes that the predation rate depends on prey abundance only, while it is independent of the inorganic nitrogen source and does not cease at high cellular nitrogen contents of the mixotroph. Conversely, however, the uptake rate of inorganic nutrient can be suppressed by the ingestion of prey via an increase of the cellular nutrient content of the mixotroph (see Eqns 3 and 6). Hence, our model assumes that the mixotroph prefers heterotrophic over autotrophic growth, in agreement with the predominantly heterotrophic nutrition of the mixotroph *Ochromonas* (Andersson et al. 1989, Sanders et al. 2001, Wilken et al. 2013b). Yet, at low prey abundances its heterotrophic lifestyle is less profitable, and the mixotroph shifts to autotrophic growth through its type III functional response.

Parameter estimates

The model was parameterized based on the settings of our chemostat experiments and a series of independent experiments with the autotroph *Microcystis aeruginosa*, the mixotroph *Ochromonas* sp., and ammonium as the limiting nutrient. In chemostats, the nutrient turnover rate D and the nutrient load N_{in} (see Eqn 1) are set by the dilution rate of the chemostat and the nutrient concentration in the mineral medium, respectively. We assume that the specific loss rates of both species were governed by the dilution rate of the chemostat (i.e., $m_A = m_M = D$). The maximum specific growth rate (μ_{max}) and maximum cellular nitrogen content (Q_{max}) of *Microcystis* were measured during exponential growth in an independent chemostat experiment provided with a saturating nitrogen concentration of 500 µM in the mineral medium. The maximum specific growth rate of *Ochromonas* was measured during exponential growth under mixotrophic conditions, by inoculation of a small amount of *Ochromonas* into the *Microcystis* chemostat experiment after *Microcystis* had reached high population densities. We were not able to measure the maximum cellular nitrogen content of *Ochromonas* during this experiment, because the *Ochromonas* cells could not be separated from the *Microcystis* cells. The minimum cellular nitrogen contents (Q_{min}) of *Microcystis* and *Ochromonas* were measured under autotrophic conditions, using nitrogen-limited batch cultures in which the cells became nitrogen-starved at the stationary phase. The functional response of *Ochromonas* grazing on *Microcystis* was obtained from the grazing experiments of Wilken et al. (2010), adopting their values for the maximum ingestion rate (f_{max}) and the curvature of the functional response (b), but using the half-saturation constant (k_M) as a tuning parameter to account for differences in predator-prey encounter rates between the batch experiments of Wilken et al. (2010) and the much more turbulent conditions in our chemostat experiments. The remaining model parameters (u_{max} and K of both species; Q_{max} of *Ochromonas*) were obtained from earlier monoculture chemostat experiments with *Microcystis aeruginosa* and *Ochromonas* sp. using ammonium as the limiting

nutrient (Wilken et al. 2013a). The parameter values are summarized in Table 1.

Model predictions

The model predictions are illustrated in Fig. 1. From these results, which are in good agreement with other intraguild predation models (Holt and Polis 1997, Diehl and Feissel 2000), we deduce the following theoretical predictions: (i) at low nutrient loads, the autotroph dominates; (ii) at intermediate nutrient loads, the autotroph and mixotroph coexist; (iii) with a further increase in nutrient loads, the mixotroph becomes dominant, while the population density of the autotroph decreases; (iv) the inorganic nutrient concentration shows a slight increase after the mixotroph has entered the system, but remains rather low; (v) the community does not show alternative stable states or non-equilibrium dynamics such as predator-prey oscillations (Fig. 1).

With respect to prediction (iii), we note that the type III functional response of the mixotroph implies that its grazing pressure on the autotroph becomes negligible when the autotroph becomes rare. Hence, the model predicts that the mixotroph will suppress the autotroph at high nutrient loads, but will not drive it to extinction (Wilken et al. 2013a). Furthermore, we note that prediction (v) is specific for our parameter estimates, while intraguild predation models can display alternative stable states and predator-prey oscillations for other parameter combinations (cf. Holt and Polis 1997; Verdy and Amarasekare 2010; Hiltunen et al. 2013).

Materials and methods

Species

Our experiments were performed with the mixotrophic chrysophyte *Ochromonas* sp. as intraguild predator, and the toxic cyanobacterium *Microcystis aeruginosa* PCC 7806 as intraguild prey. *Microcystis* PCC 7806 is a single-celled strain producing the hepatotoxin microcystin-LR. It

has a cellular biovolume of 29.6 (± 1.0 SD) μm^3, and did not show any colony formation during the experiments. Our *Ochromonas* strain is probably *Ochromonas globosa* Skuja (determined by Dr R. Bijkerk, Koeman & Bijkerk B.V., Ecological Research and Advice, Haren, The Netherlands). It was originally detected as infection in a large-scale mesocosm experiment with *Microcystis*, from which it was isolated with micro-needle techniques (Van Donk et al. 2009). Its cellular biovolume is 211.9 (± 21.9 SD) μm^3. We showed in earlier experiments that this *Ochromonas* strain can feed effectively on *Microcystis*, and is not affected by its toxin microcystin (Wilken et al. 2010).

Chemostat experiments

The theoretical predictions were tested in chemostat experiments, using three different nitrogen concentrations in the mineral medium (N_{in} = 20, 100 and 500 µM of NH_4Cl) to generate an experimental productivity gradient. These concentrations reflect the range of total nitrogen concentrations typically found in eutrophic lakes with dense *Microcystis* blooms (Verspagen et al. 2006; Jöhnk et al. 2008; Xu et al. 2010). All other nutrients were provided in excess using a nutrient-rich mineral medium (Wilken et al. 2013b). First, monoculture chemostats of *Microcystis* and *Ochromonas* were grown at each nitrogen level. After the monocultures had been maintained at steady state for at least two weeks, mixed cultures were produced by cross-inoculating each monoculture with 5% from the monoculture of the other species at the same nitrogen level. This resulted in two mixed cultures at each nitrogen level, one in which a small amount of *Ochromonas* was added to a steady-state monoculture of *Microcystis* and the other in which a small amount of *Microcystis* was added to a steady-state monoculture of *Ochromonas*. Hence, this procedure provided a straightforward method to test for alternative stable states.

The chemostat experiments were performed in 1.6 L flat culture vessels as described in Huisman et al. (1999, 2002), with a dilution rate of $D = 0.12$ d^{-1}. The temperature was kept constant at 23 ± 1 °C by a metal cooling finger connected to a water bath. Light was supplied by white fluorescent tubes (Philips PL-L 24W/840/4P, Eindhoven, The Netherlands) at a constant incoming irradiance (I_{in}) of 50 ± 2 µmol photons m^{-2} s^{-1}. The chemostats were aerated with filter-sterilized air at a flow rate of 20 L/h. To prevent introduction of gaseous ammonium, the air flow was cleaned by leading it through a 0.5 N phosphoric acid solution before entering the chemostat cultures. The photosynthetic activity of dense cultures may deplete the CO_2 concentration and raise the pH. Therefore, the pH was continuously monitored, and carbon limitation was avoided by enriching the air flow with adjustable concentrations of CO_2 using Brooks Mass Flow Controllers (Brooks Instruments, Hatfield, PA, USA), targeted to stabilize the pH at 7.8. Wall growth was removed daily by scraping the walls with a magnetic stirrer.

The chemostats were sampled approximately every other day. Samples for cell counts were fixed with a mixture of glutaraldehyde and formaldehyde (final concentration of 0.025 and 0.0037 percent by mass, respectively) and stored at 4 °C until counting at a flow cytometer (MoFlo XDP cell sorter, Beckman Coulter, Miami, FL, USA). The flow cytometer distinguished between *Ochromonas* and *Microcystis* based on their cell size and pigmentation. Samples for determination of the dissolved ammonium concentration were centrifuged for 10 min at 4,000 rpm and the supernatant was stored at -20 °C until further analysis. Ammonium concentrations were measured using the fluorometric method described in Holmes et al. (1999). To determine particulate organic carbon and nitrogen concentrations, cultures were filtered onto pre-combusted glassfibre filters (Whatman GF/F), dried at 60 ºC overnight, and measured using an Elemental Analyzer (Flash 2000; Thermo Fisher Scientific, Waltham, MA, USA). We also calculated the cellular nitrogen content from the difference between the dissolved inorganic nitrogen

concentration in the mineral medium and in the chemostat vessel using mass balance considerations. The incident light intensity (I_{in}) and the light intensity transmitted through the chemostat vessel (I_{out}) were measured for at least 6 time points during steady state of both monocultures and mixed cultures. Measurements were performed with a LI-COR LI-250 quantum photometer (LI-COR Biosciences, Lincoln, NE, USA) at 10 randomly chosen positions on the front and back surface of the chemostat vessel, respectively. The depth-averaged light intensity in the cultures (I_{avg}) can then be calculated as $I_{avg}=(I_{in}-I_{out})/(\ln[I_{in}]-\ln[I_{out}])$ (Huisman et al. 2002).

Results

Chemostat experiments

The autotroph *Microcystis* and the mixotroph *Ochromonas* both grew well in monoculture, and increased in abundance with increasing nitrogen load (Fig. 2). *Ochromonas* had a lower growth rate than *Microcystis*, as can be seen from the longer time span needed until steady state was reached (compare Fig. 2E and F). Due to its smaller cell size, the cellular nitrogen content of *Microcystis* was lower than that of *Ochromonas*, reaching steady-state values of 0.034-0.038 pmol cell^{-1} in *Microcystis* as compared to 0.26-0.32 pmol cell^{-1} in *Ochromonas*. Consequently, *Microcystis* reached about 10-fold higher steady-state abundances than *Ochromonas* (Fig. 2; Fig. 3A). The measured cellular nitrogen contents were in good agreement with the steady-state values of 0.038 pmol cell^{-1} for *Microcystis* and 0.27 pmol cell^{-1} for *Ochromonas* predicted by the model.

The linear increase in steady-state abundance of both species with increasing nitrogen load confirmed that nitrogen was indeed the limiting factor, even at the highest nitrogen level (Fig. 3A). Furthermore, *Microcystis* cells showed high C/N-ratios of ~17 at all nitrogen loads (Fig

3B). C/N-ratios of *Ochromonas* were lower, especially at 100 and 500 µM N load, but also remained well above the Redfield ratio of 6.6. The depth-averaged light intensity was slightly reduced to $I_{avg} \approx 33$ µmol photons m^{-2} s^{-1} in the cultures provided with high nitrogen loads (Fig. 3B), indicative of mild self-shading by the increasing population abundances. At steady state, *Microcystis* reduced the dissolved ammonium concentration to lower levels than *Ochromonas* (paired t-test: t_2=5.05, P<0.05; Fig. 3C). Hence, *Microcystis* has a lower critical ammonium concentration (i.e., a lower R^* sensu Tilman 1982), and resource competition theory therefore predicts that *Microcystis* will be the better competitor for ammonium (Grover 1991, Smith and Waltman 1994).

After inoculation of *Microcystis* into the monocultures of *Ochromonas*, the *Microcystis* abundance remained low for several weeks and then slowly increased (Fig. 4A,C,E). At low nitrogen load, the *Ochromonas* population was not much affected by the invasion of *Microcystis* (Fig. 4A). However, at intermediate and high nitrogen load, the increase of *Microcystis* came along with a clear decline in *Ochromonas* abundance (Fig. 4C,E). Conversely, after inoculation of *Ochromonas* into the *Microcystis* monocultures, *Ochromonas* showed high initial grazing rates on the *Microcystis* populations, resulting in a rapid increase of the *Ochromonas* population. *Microcystis* quickly declined within the first 1-2 weeks, from 450,000 to less than 1,000 cells/mL at the low nitrogen load (Fig. 4B), from 2.6 million to 50,000 cells/mL at the intermediate nitrogen load (Fig. 4D), and from 12 million to 300,000 cells/mL at the high nitrogen load (Fig. 4F). Hence, within the first few weeks *Microcystis* was reduced by > 97% at all three nutrient treatments. After some time, however, the growth rates of *Ochromonas* dwindled, and concomitantly *Microcystis* was able to slowly grow up again (Fig. 4B,D,F). Steady-state abundances of *Ochromonas* and *Microcystis* converged to similar levels, irrespective of whether the species mixtures were started from the *Ochromonas* or *Microcystis* monocultures (compare

left column versus right column in Fig. 4). This indicates that the outcome of the species interactions was independent of the initial conditions. The species abundances at high nitrogen load seemed to fluctuate mildly, suggestive of small-amplitude predator-prey oscillations (Fig. 4E,F). The dissolved ammonium concentration remained low in all treatments.

In the species mixtures, both *Ochromonas* and *Microcystis* increased in steady-state abundance with increasing nitrogen load (Fig. 5A). At the lowest nitrogen load, *Ochromonas* reached slightly higher steady-state abundances than in monoculture and suppressed *Microcystis* by 80% relative to its monoculture abundance (Fig. 5B). Hence, the mixotroph was facilitated by the presence of its prey at low nitrogen loads. In contrast, at the intermediate and high nitrogen loads *Ochromonas* reached lower steady-state abundances than in monoculture, while *Microcystis* was suppressed by only 40-50%. Thus, although both species increased with the nitrogen load, the intraguild prey *Microcystis* benefitted relatively more from the increasing nitrogen load than its intraguild predator *Ochromonas*. As in the monocultures, the depth-averaged light intensity was slightly reduced at high nitrogen loads, indicative of mild shading (Fig. 5C). Due to their similarity in size the two species could not be separated from the mixture, and hence, the C/N ratio could not be determined for each species individually. The C/N ratio of the species mixtures was intermediate between the C/N ratios of the monocultures of *Microcystis* and *Ochromonas* (compare Fig. 3B and 5C). Likewise, the dissolved ammonium concentration in the species mixture was slightly higher than in the *Microcystis* monocultures, while it was slightly lower than in the *Ochromonas* monocultures (Fig. 5D; Friedmann ANOVA X^2=2.67, df=2, P=0.26).

Evaluation of theoretical predictions

We can now evaluate to what extent the theoretical predictions are supported by the experiments:

Prediction (i): at low nutrient load, the autotroph dominates. The autotroph *Microcystis* was not the dominant species at the lowest nutrient load of 20 μM. In fact, the mixotroph *Ochromonas* strongly suppressed its autotrophic prey (Fig. 4A,B). However, the parameterized model predicts dominance of the autotroph only at very low nitrogen loads of $N_{in} < 2$ μM, but coexistence of the autotroph and mixotroph at higher nitrogen loads (Fig. 1). Hence, the applied nutrient load of 20 μM was apparently not low enough to enable dominance of the autotroph.

Prediction (ii): at intermediate nutrient load, the autotroph and mixotroph coexist. This prediction is supported by the experiments.

Prediction (iii): with a further increase in nutrient load, the mixotroph becomes dominant while the autotroph decreases in abundance. This prediction is not supported. The autotroph and mixotroph both increased in abundance with the nutrient load (Fig. 5A). In relative terms, the dominance of the mixotroph *Ochromonas* even decreased and the autotroph *Microcystis* was suppressed less strongly at high nutrient loads (Fig. 5B).

Prediction (iv): the dissolved inorganic nutrient concentration slightly increases after the mixotroph has entered the system, but remains rather low. As predicted, there was a slight increase in the dissolved ammonium concentration in the species mixtures compared to the *Microcystis* monocultures, but the ammonium concentrations clearly remained low in all experiments.

Prediction (v): the community does not show alternative stable states or predator-prey oscillations. Despite completely different initial conditions, the two experiments at each nutrient level rapidly converged to the same population dynamics. Hence, we did not find evidence for alternative stable states. The population dynamics suggest convergence to equilibrium at low nutrient load, but mild predator-prey oscillations at high nutrient load.

Summarizing, several of the model predictions are supported by the experiments. However, the experimental results clearly contradict the expectation based upon prediction (iii) that mixotrophs (intraguild predators) will dominate at high nutrient loads, while autotrophs (intraguild prey) will decrease with increasing nutrient loads.

Explanations for the discrepancy between theory and experiments

Similar to our findings, earlier studies have been puzzled by the persistence of intraguild prey species in productive environments (Holt and Polis 1997, Amarasekare 2007). This has recently inspired a series of theoretical papers analyzing possible mechanisms that allow coexistence of intraguild predators and their prey (Křivan and Diehl 2005, Finke and Denno 2006, Janssen et al. 2007, Amarasekare 2008, Abrams and Fung 2010, Urbani and Ramos-Jiliberto 2010, Hin et al. 2011). However, only very few studies have tested these mechanisms experimentally (e.g., Amarasekare 2007). Here, we experimentally explore several potential mechanisms to find a suitable explanation for the observed lack of biological control of the intraguild prey population at high nitrogen loads. Detailed descriptions of the experimental methods can be found in Appendix A.

(i) Genetic diversity within the prey: Genetic variation within the prey population can result in rapid prey evolution (Yoshida et al. 2003), and may select for predator-resistant genotypes that allow persistence of the prey at high predator densities (Meyer et al. 2006). We therefore tested for genetic variation in the *Microcystis* population using denaturing gradient gel electrophoresis (DGGE) of three different parts of the internal transcribed spacer (ITS) between the 16S and 23S rRNA coding regions. This approach allows detection of different *Microcystis* strains at high resolution (Janse et al. 2003; Kardinaal et al. 2007a). Samples from our chemostat resulted in only one band in the DGGE gel, confirming the presence of only the strain PCC 7806

368 in the chemostats (Fig. 6). Hence, we did not detect genetic variation within the *Microcystis*
369 population, at least not at the ITS region. We note that some degree of mutation-derived genetic
370 variation might also occur within a clonal culture and would escape detection by DGGE of the
371 ITS region. Yet, it seems unlikely that *de novo* mutations during the experiments can explain our
372 results, because the similarity of the trajectories in the different chemostats indicates that this
373 would require similar mutations at almost the same time points in several independent
374 chemostats. Hence, although we cannot exclude the possibility of prey evolution in our
375 chemostats, it does not seem to be a very plausible explanation of our results.

376 *(ii) Inducible defenses within the prey:* Predator resistance can also be induced as a
377 phenotypic response of the prey to enhanced predation pressure. Such inducible defenses can
378 prevent oscillations in predator-prey systems (Verschoor et al. 2004) and may enable intraguild
379 prey to coexist with their intraguild predators at high levels of productivity (Abrams and Fung
380 2010, Urbani and Ramos-Jiliberto 2010). We used a standard protocol to test for inducible
381 defenses (Hessen and Van Donk 1993), in which we exposed the intraguild prey *Microcystis* to
382 the filtrates of other *Microcystis* cultures grown either with or without *Ochromonas* as grazer. In
383 case of an inducible defense, one would expect a lower grazing rate on the 'induced' *Microcystis*.
384 However, grazing rates were about 20 % higher on the 'induced' *Microcystis* than on the control
385 (Student's t-test: t_4=-7.53, $p<0.005$; data not shown). Thus, there was no evidence for an
386 inducible defense against grazing in *Microcystis*.

387 *(iii) Changes in nutritional quality of the prey:* The nutritional quality of prey species may
388 vary along nutrient gradients (Sterner and Elser 2002, Andersen et al. 2004). Because predatory
389 chrysophytes can alter their grazing rates in response to changes in the nitrogen content of their
390 prey (John and Davidson 2001), we tested whether nitrogen deprivation of the intraguild prey
391 *Microcystis* affected the performance of its predator *Ochromonas*. The results show that nitrogen

deprivation caused a clear decrease of the cellular nitrogen content of *Microcystis* (Fig. 7A). Although this did not lead to a decrease in grazing rate (Fig. 7B), it strongly suppressed the growth rate of *Ochromonas* on N-deprived *Microcystis* cells (Fig. 7C). This suggests, however, that *Ochromonas* will be a weaker predator at low nitrogen loads, whereas our chemostat experiments indicated a reduced predation pressure at high nitrogen loads. Hence, it seems unlikely that such a change in nutritional quality of *Microcystis* can explain the observed patterns in population abundance.

(iv) A shift towards competition for light: An increase in nutrient load allows accumulation of higher biomass, which reduces light availability due to self-shading, and may shift the species interactions from competition for nutrients to competition for light (Passarge et al. 2006, Brauer et al. 2012). Assuming that the autotroph *Microcystis* is the better competitor for light, this may tend to favor *Microcystis* at high nitrogen loads. Light limitation might furthermore result in lower grazing rates by the mixotroph (Li et al. 1999), and thus reduce the grazing pressure on *Microcystis*. However, the linear increase in population density with nitrogen load provides strong evidence that nitrogen was the limiting factor across all nitrogen levels that we applied (Fig. 3A). This is further supported by the consistently high C/N ratio of *Microcystis* of ~17 (Fig. 3B). This high C/N ratio is typical for nitrogen-limited growth of *Microcystis*, while it is known to have a much lower C/N ratio of 6-7 under light-limited conditions (Van de Waal et al. 2009). The depth-averaged light intensity was slightly reduced in the chemostats receiving the highest nitrogen load (Fig. 3B and 5C), but this mild degree of self-shading seems insufficient to shift the species interactions to competition for light. For comparison, dense chemostat cultures with lots of self-shading reduce I_{avg} to much lower values under light-limited conditions (e.g., Huisman et al. 1999; Passarge et al. 2006; Kardinaal et al. 2007b; Van de Waal et al. 2009). As a final piece of evidence to corroborate the absence of light limitation, we increased the light

supply (I_{in}) for the chemostats with the highest nitrogen load to reach the same depth-averaged light intensity as in the chemostats with lower nitrogen loads. The time point at which the light supply was increased is indicated by the vertical dotted line in Fig. 4E and F. The results show that an increase in the light supply did not affect the steady-state abundances of the species. Hence, we conclude that even the chemostat experiments at the highest nitrogen load were nitrogen-limited rather than light-limited. A shift towards competition for light is therefore unlikely to explain the observed increase of the *Microcystis* population with nutrient enrichment.

(v) Intraspecific interference within the predator population: Grazing rates of the predators may depend not only on prey abundance, but may also change with the abundance of the predator. For instance, grazing rates may decrease with increasing predator abundances due to intraspecific interference within the predator population, which may allow coexistence of the intraguild predator and prey at high levels of productivity (Amarasekare 2008). In mixotrophic populations, physical interactions among the individuals might interfere with the ingestion of prey, while nutrient uptake by mixotrophs is less likely to be affected by interference. Because we observed physical interactions among *Ochromonas* individuals under the microscope, we tested for intraspecific predation interference within *Ochromonas* by investigating the dependence of its grazing rates on its own population density. This confirmed that grazing rates decreased at high abundances of *Ochromonas* (Fig. 8). These results suggest that intraspecific predation interference might explain the reduced predation pressure of *Ochromonas* on *Microcystis* at high nitrogen loads.

To explore this possible explanation in further detail, we rewrote the type III functional response to account for intraspecific interference among the predators (DeAngelis et al. 1975, Skalski and Gilliam 2001):

$$f_M(A,M) = \frac{f_{\max}(A/k_M)^b}{1+(A/k_M)^b + cM} \quad (9)$$

The functional response thus becomes a function $f_M(A,M)$ of the abundances of both the autotroph and mixotroph. The parameter c determines the strength of the interference. We fitted c by minimization of the residual sum of squares using the Gauss-Marquardt-Levenberg algorithm in the software package PEST (Watermark Numerical Computing, Brisbane, Australia). All other parameters remained the same as in Table 1. Compared to the original model without predation interference (Fig. 9A), the incorporation of predation interference resulted in a much better fit of the model to our experimental data (Fig. 9B). In particular, the model predicts that predation interference will enable a strong increase of the autotroph *Microcystis* with increasing nutrient loads, in line with our observations. Therefore, interference within the intraguild predator population offers a possible explanation for the discrepancy between the experimental results and the theoretical expectations.

Discussion

Our experimental results show that the mixotroph *Ochromonas* effectively suppressed the toxic cyanobacterium *Microcystis* at low nutrient loads, but not at high nutrient loads. Instead, *Microcystis* and its mixotrophic predator coexisted across the entire productivity range applied in our experiments. Based on intraguild predation theory, a necessary (but not sufficient) condition for coexistence is that the autotrophic prey *Microcystis* is the better competitor for the shared resource (Holt and Polis 1997). Indeed, *Microcystis* had a lower critical ammonium concentration (i.e., a lower R^*) than *Ochromonas* during autotrophic growth (Fig. 3C), and hence is the better competitor for ammonium (Tilman 1982, Smith and Waltman 1994). The lower competitive strength of *Ochromonas* might reflect the high costs of mixotrophic growth, which requires

462 investments into the biochemical machinery for both autotrophic and heterotrophic nutrition
463 (Raven 1997).

464 Our results contradict the model prediction that the intraguild prey would be more
465 strongly suppressed with increasing nutrient load, which is widely regarded as one of the key
466 predictions of intraguild predation theory (Holt and Polis 1997, Diehl and Feissel 2000, Mylius et
467 al. 2001). Its function as intraguild predator enabled *Ochromonas* to strongly suppress
468 *Microcystis* at the lowest nitrogen load. However, although *Ochromonas* increased in abundance
469 with a further increase in nitrogen load, this did not result in a stronger suppression of its prey.
470 Instead, the autotrophic prey *Microcystis* increased in abundance with increasing nutrient load,
471 both in absolute terms and relative to its abundance in monoculture (Fig. 5A,B). The ability of
472 *Ochromonas* to suppress *Microcystis* therefore declined at high nitrogen loads.

473 Motivated by earlier studies aiming to explain the frequently observed coexistence of
474 intraguild prey and predator species (e.g., Liess and Diehl 2006, Amarasekare 2008, Abrams and
475 Fung 2010, Urbani and Ramos-Jiliberto 2010), we explored a number of potential explanations
476 for our experimental results. One interesting aspect of our experiments is that the intraguild
477 predator *Ochromonas* uses a type III functional response (Wilken et al. 2010), whereas most
478 previous theory developed for intraguild predation assumed a type I or type II functional response
479 (e.g., Holt and Polis 1997, Diehl and Feissel 2000; but see Gismervik and Andersen 1997). The
480 type III functional response indicates that *Ochromonas* switches to autotrophic growth when prey
481 becomes rare, which reduces the per capita mortality rate of the prey species. As a consequence, a
482 type III functional response enables persistence of the intraguild prey irrespective of the nutrient
483 load. Yet, despite its persistence, the model predicts that incorporation of the type III response
484 will still lead to a reduction in prey abundance with increasing nutrient load (Fig. 1). Hence, the
485 type III response is not sufficient to explain the experimental results. Furthermore, we did not

find experimental evidence for several other possible explanations for the observed pattern, such as genetic diversity within the prey, inducible defenses, a reduced nutritional quality, or a shift from competition for nutrient to competition for light. However, we did find experimental support for intraspecific interference within the *Ochromonas* population, which reduced the grazing rate upon *Microcystis* when *Ochromonas* became more abundant.

Intraspecific interference can suppress the extent to which predator populations increase with nutrient enrichment and has been reported by several zooplankton studies. For example, chemical interference is believed to cause intraspecific density dependence in small cladocerans, while cannibalism has been noted on naupliar stages of copepods (Declerck et al. 2003, Basedow and Tande 2006). Intraspecific interference among the intraguild predator would explain several of our findings. First, given the high ingestion rates that *Ochromonas* can achieve when grazing on *Microcystis*, it should be able to control *Microcystis* growth even at the abundances reached in our experiment. The inability to control *Microcystis* more strongly can therefore not simply be ascribed to an inability of *Ochromonas* to reach higher abundances; something must have suppressed its grazing rate. Second, at the higher nutrient loads, *Ochromonas* reached lower abundances as intraguild predator in the species mixture than as autotroph in monoculture (Fig. 5B). This is rather counterintuitive, because one would expect that addition of prey to an autotrophically growing mixotroph should increase its population abundance, especially if the mixotroph has a preference for heterotrophic growth. Our interpretation of this counterintuitive result is that (i) *Microcystis* is the better competitor for ammonium and thereby suppresses opportunities for autotrophic growth of *Ochromonas*, while (ii) at high population abundances *Ochromonas* cannot graze efficiently on *Microcystis* due to intraspecific interference. Third, model simulations show that predation interference indeed leads to a relatively strong increase of the autotroph with increasing nutrient loads, in line with our experimental results. Therefore,

510 interference within the intraguild predator population offers a plausible mechanism for the
511 inability of *Ochromonas* to suppress *Microcystis* at high nutrient loads.

512 However, the list of mechanisms we tested experimentally is not exhaustive and we can
513 therefore not exclude other factors that were not investigated. For instance, the temporal
514 dynamics suggest a slow decrease in grazing pressure before *Microcystis* abundances started to
515 increase again in the mixed cultures (Fig. 4). It could well be that, due to genotypic or phenotypic
516 changes, *Ochromonas* might have inactivated part of its cellular machinery for heterotrophic
517 metabolism once *Microcystis* was suppressed to sufficiently low abundances. That is,
518 *Ochromonas* might have shifted its trophic position from an intraguild predator to a
519 predominantly autotrophic competitor during the experiment. Since *Ochromonas* is a weaker
520 competitor for ammonium than *Microcystis*, this might explain the initial decline and subsequent
521 partial recovery of the *Microcystis* populations observed in several of the experiments (Fig.
522 4B,D,F). While evolution of the nutritional strategy of mixotrophs has been shown
523 experimentally (Reboud and Bell 1997, Bell 2013), we have not developed new theory or ran
524 additional experiments to investigate such alternative explanations in further detail.

525 Natural communities offer a much more complex setting than our experimental system.
526 The abundance of *Ochromonas* is typically lower in natural communities than in our chemostat
527 experiments (Van Donk et al. 2009), which will most likely reduce the importance of predation
528 interference due to lower encounter rates among *Ochromonas* individuals. However, other factors
529 preventing control of *Ochromonas* over its intraguild prey might become more important in
530 natural waters. For instance, although our *Microcystis* strain remained single-celled, *Ochromonas*
531 is known to induce colony formation in some other strains of *Microcystis* (Burkert et al. 2001),
532 and the large *Microcystis* colonies often observed in eutrophic lakes offer efficient protection
533 against grazing by *Ochromonas* (Yang and Kong 2012). In addition, grazing by protists can act as

534 selection factor on *Microcystis* populations, and evolution towards less edible strains is likely to
535 occur in natural populations (Van Wichelen et al. 2010). Furthermore, in their natural habitat
536 *Ochromonas* and *Microcystis* will not interact in isolation. *Ochromonas* can utilize alternative
537 prey organisms, such as heterotrophic bacteria (Wilken et al. 2013b), while both species are
538 subject to predation by and competition with other species. All these aspects may affect the
539 abundance patterns of *Microcystis* and *Ochromonas* along natural productivity gradients.
540 Nutrient enrichment of aquatic ecosystems, through agriculture, urbanization, and other
541 human activities, has increased the risk of toxic cyanobacterial blooms (Chorus and Bartram
542 1999, Huisman et al. 2005, Paerl and Huisman 2008). To what extent can mixotrophic species
543 like *Ochromonas* suppress or even prevent cyanobacterial bloom development? Our experiments
544 showed that *Ochromonas* initially reduced the abundance of the toxic cyanobacterium
545 *Microcystis* by more than 97%. After several weeks, however, *Microcystis* partially recovered to
546 about 20% of its original monoculture abundance at low nitrogen loads, and to about 50-60% of
547 its monoculture abundance at high nitrogen loads. Furthermore, in previous experiments we
548 showed that *Ochromonas* cannot grow on nitrate, and therefore *Ochromonas* is capable to
549 suppress *Microcystis* populations much more strongly with ammonium than with nitrate as
550 nitrogen source (Wilken et al2013a). Taken together, these findings suggest that mixotrophic
551 chrysophytes like *Ochromonas* are most effective as biological control agents of toxic
552 cyanobacteria in relatively oligotrophic waters with ammonium as the dominant nitrogen source.
553 In eutrophic waters, where the problem of cyanobacterial blooms is generally most severe, a
554 newly invading *Ochromonas* population may have a transient effect but will ultimately have less
555 control over cyanobacterial populations.
556 In conclusion, while intraguild predators may act as effective biological control agents
557 against pest species, our study highlights the potential of several mechanisms to reduce this

558 control. Understanding the relative importance of these mechanisms is crucial to make
559 predictions about the possibilities for biological control in specific communities. The mixotroph
560 *Ochromonas* is capable of strongly suppressing toxic cyanobacteria at low nutrient loads, but
561 intraspecific predation interference is one of the mechanisms preventing its control over toxic
562 cyanobacteria at high nutrient loads. Hence, although *Ochromonas* does reduce the harmful
563 cyanobacterium *Microcystis* to some extent, it is unlikely to be a very effective biological control
564 agent against toxic cyanobacterial blooms in eutrophic waters.
565

566 **Acknowledgments**

567 We thank the anonymous reviewers for their helpful comments. We are grateful to N.
568 Helmsing for carbon measurements and to A. Steenbergh for help with DGGE. This study was
569 supported by the Netherlands Institute of Ecology (NIOO-KNAW) and by the Earth and Life
570 Sciences Foundation (ALW), which is subsidized by the Netherlands Organization for Scientific
571 Research (NWO). This is publication no. 5548 of the Netherlands Institute of Ecology (NIOO-
572 KNAW).
573

Literature cited

Abrams, P. A., and S. R. Fung. 2010. The impact of adaptive defence on top-down and bottom-up effects in systems with intraguild predation. Evolutionary Ecology Research 12:307-325.

Amarasekare, P. 2007. Trade-offs, temporal variation, and species coexistence in communities with intraguild predation. Ecology 88:2720-2728.

Amarasekare, P. 2008. Coexistence of intraguild predators and prey in resource-rich environments. Ecology 89:2786-2797.

Andersen, T., J. J. Elser, and D. O. Hessen. 2004. Stoichiometry and population dynamics. Ecology Letters 7:884-900.

Andersson, A., S. Falk, G. Samuelsson, and A. Hagström. 1989. Nutritional characteristics of a mixotrophic nanoflagellate, *Ochromonas* sp. Microbial Ecology 17:251-262.

Arim, M., and P. A. Marquet. 2004. Intraguild predation: a widespread interaction related to species biology. Ecology Letters 7:557-564.

Bampfylde, C. J., and M. A. Lewis. 2007. Biological control through intraguild predation: case studies in pest control, invasive species and range expansion. Bulletin of Mathematical Biology 69:1031-1066.

Basedow, S. L., and K. S. Tande. 2006. Cannibalism by female *Calanus finmarchicus* on naupliar stages. Marine Ecology Progress Series 327:247-255.

Bell, G. 2013. Experimental evolution of heterotrophy in a green alga. Evolution 67:468–476.

Borer, E. T., C. J. Briggs, W. W. Murdoch, and S. L. Swarbrick. 2003. Testing intraguild predation theory in a field system: does numerical dominance shift along a gradient of productivity? Ecology Letters 6:929-935.

596 Brauer, V. S., M. Stomp, and J. Huisman. 2012. The nutrient-load hypothesis: patterns of
597 resource limitation and community structure driven by competition for nutrients and light.
598 American Naturalist 179**:**721-740.
599 Burkert, U., P. Hyenstrand, S. Drakare, and P. Blomqvist. 2001. Effects of the mixotrophic
600 flagellate *Ochromonas* sp. on colony formation in *Microcystis aeruginosa*. Aquatic
601 Ecology 35:9-17.
602 Burkholder, J. M., P. M. Glibert, and H. M. Skelton. 2008. Mixotrophy, a major mode of
603 nutrition for harmful algal species in eutrophic waters. Harmful Algae 8:77-93.
604 Carmichael, W. W., S. M. F. O. Azevedo, J. S. An, R. J. R. Molica, E. M. Jochimsen, S. Lau, K.
605 L. Rinehart, G. R. Shaw, G. K. Eaglesham. 2001. Human fatalities from cyanobacteria:
606 chemical and biological evidence for cyanotoxins. Environmental Health Perspectives
607 109:663-668.
608 Chorus, I., and J. Bartram. 1999. Toxic cyanobacteria in water: a guide to their public health
609 consequences, monitoring and management. E and FN Spon, London, UK.
610 Codd, G. A. 1995. Cyanobacterial toxins: occurrence, properties and biological significance.
611 Water Science and Technology 32:149-156.
612 Codd, G. A., L. F. Morrison, and J. S. Metcalf. 2005. Cyanobacterial toxins: risk management for
613 health protection. Toxicology and Applied Pharmacology 203:264-272.
614 DeAngelis, D. L., R. A. Goldstein, and R. V. ONeill. 1975. A model for trophic interaction.
615 Ecology 56:881-892.
616 Declerck, S., V. Geenens, N. Podoor, J. M. Conde Porcuna, and L. De Meester. 2003.
617 Intraspecific density dependence in the dynamics of zooplankton under hypertrophic
618 conditions. Canadian Journal of Fisheries and Aquatic Sciences 60:919-928.

619 Diehl, S., and M. Feissel. 2000. Effects of enrichment on three-level food chains with omnivory.
620 American Naturalist 155:200-218.
621 Diehl, S., and M. Feissel. 2001. Intraguild prey suffer from enrichment of their resources: a
622 microcosm experiment with ciliates. Ecology 82:2977-2983.
623 Droop, M. R. 1973. Some thoughts on nutrient limitation in algae. Journal of Phycology 9:264-
624 272.
625 Ducobu, H., J. Huisman, R. R. Jonker, and L. R. Mur. 1998. Competition between a
626 prochlorophyte and a cyanobacterium under various phosphorus regimes: comparison
627 with the Droop model. Journal of Phycology 34:467-476.
628 Finke, D. L., and R. Denno. 2006. Predator diversity and the functioning of ecosystems: the role
629 of intraguild predation in dampening trophic cascades. Ecology Letters 8:1299-1306.
630 Flynn, K. J., D. K. Stoecker, A. Mitra, J. A. Raven, P. M. Glibert, P. J. Hansen, E. Granéli, and J.
631 M. Burkholder. 2013. Misuse of the phytoplankton-zooplankton dichotomy: the need to
632 assign organisms as mixotrophs within plankton functional types. Journal of Plankton
633 Research 35:3-11.
634 Gismervik, I., and T. Andersen. 1997. Prey switching by *Acartia clausi*: experimental evidence
635 and implications of intraguild predation assessed by a model. Marine Ecology Progress
636 Series 157:247-259.
637 Grover, J. P. 1991. Resource competition in a variable environment: phytoplankton growing
638 according to the variable-internal-stores model. American Naturalist 138:811-835.
639 Hartmann, M., C. Grob, G. A. Tarran, A. P. Martin, P. H. Burkill, D. J. Scanlan, and M. V.
640 Zubkov. 2012. Mixotrophic basis of Atlantic oligotrophic ecosystems. Proceedings of the
641 National Academy of Sciences USA 109:5756-5760.

642 Hessen, D. O., and E. Van Donk. 1993. Morphological changes in *Scenedesmus* induced by
643 substances released from *Daphnia*. Archiv für Hydrobiologie 127:129-140.
644 Hiltunen, T., L. E. Jones, S. P. Ellner, and N. G. Hairston Jr. 2013. Temporal dynamics of a
645 simple community with intraguild predation: an experimental test. Ecology 94:773-779.
646 Hin, V., T. Schellekens, L. Persson, and A. M. de Roos. 2011. Coexistence of predator and prey
647 in intraguild predation systems with ontogenetic niche shifts. American Naturalist
648 178:701-714.
649 Holmes, R. M., A. Aminot, R. Kerouel, B. A. Hooker, and B. J. Peterson. 1999. A simple and
650 precise method for measuring ammonium in marine and freshwater ecosystems. Canadian
651 Journal of Fisheries and Aquatic Sciences 56:1801-1808.
652 Holt, R. D., and G. A. Polis. 1997. A theoretical framework for intraguild predation. American
653 Naturalist 149:745-764.
654 Huisman, J., R. R. Jonker, C. Zonneveld, and F. J. Weissing. 1999. Competition for light between
655 phytoplankton species: experimental tests of mechanistic theory. Ecology 80:211-222.
656 Huisman, J., H. C. P. Matthijs, P. M. Visser, H. Balke, C. A. M. Sigon, J. Passarge, F. J.
657 Weissing, and L. R. Mur. 2002. Principles of the light-limited chemostat: theory and
658 ecological applications. Antonie van Leeuwenhoek 81:117-133.
659 Huisman, J., H. C. P. Matthijs, and P. M. Visser. 2005. Harmful cyanobacteria. Springer,
660 Dordrecht, The Netherlands.
661 Isaksson, A. 1998. Phagotrophic phytoflagellates in lakes: a literature review. Archiv für
662 Hydrobiologie, Special Issues Advances in Limnology 51:63-90.
663 Janse, I., M. Meima, W. E. A. Kardinaal, and G. Zwart. 2003. High-resolution differentiation of
664 cyanobacteria by using rRNA-internal transcribed spacer denaturing gradient gel
665 electrophoresis. Applied and Environmental Microbiology 69:6634-6643.

666 Janssen, A., M. W. Sabelis, S. Magalhães, M. Montserrat, and T. van der Hammen. 2007. Habitat
667 structure affects intraguild predation. Ecology 88:2713-2719.
668 John, E. H., and K. Davidson. 2001. Prey selectivity and the influence of prey carbon:nitrogen
669 ratio on microflagellate grazing. Journal of Experimental Marine Biology and Ecology
670 260:93-111.
671 Jöhnk, K. D., J. Huisman, J. Sharples, B. Sommeijer, P. M. Visser, and J. M. Stroom. 2008.
672 Summer heatwaves promote blooms of harmful cyanobacteria. Global Change Biology
673 14:495-512.
674 Jones, R. I. 2000. Mixotrophy in planktonic protists: an overview. Freshwater Biology 45:219-
675 226.
676 Kardinaal, W. E. A., I. Janse, M. Kamst-van Agterveld, M. Meima, J. Snoek, L. R. Mur, J.
677 Huisman, G. Zwart, and P. M. Visser. 2007a. *Microcystis* genotype succession in relation
678 to microcystin concentrations in freshwater lakes. Aquatic Microbial Ecology 48:1-12.
679 Kardinaal, W. E. A., L. Tonk, I. Janse, S. Hol, P. Slot, J. Huisman, and P. M. Visser. 2007b.
680 Competition for light between toxic and nontoxic strains of the harmful cyanobacterium
681 *Microcystis*. Applied and Environmental Microbiology 73:2939-2946.
682 Křivan, V., and S. Diehl. 2005. Adaptive omnivory and species coexistence in tri-trophic food
683 webs. Theoretical Population Biology 67:85-99.
684 Li, A., D. K. Stoecker, and J. E. Adolf. 1999. Feeding, pigmentation, photosynthesis and growth
685 of the mixotrophic dinoflagellate *Gyrodinium galatheanum*. Aquatic Microbial Ecology
686 19:163-176.
687 Liess, A., and S. Diehl. 2006. Effects of enrichment on protist abundances and bacterial
688 composition in simple microbial communities. Oikos 114:15-26.

689 Meyer, J. R., S. P. Ellner, N. G. Hairston, L. E. Jones, and T. Yoshida. 2006. Prey evolution on
690 the time scale of predator-prey dynamics revealed by allele-specific quantitative PCR.
691 Proceedings of the National Academy of Sciences USA 103:10690-10695.
692 Montserrat, M., S. Magalhães, M. W. Sabelis, A. M. de Roos, A. Janssen. 2008. Patterns of
693 exclusion in an intraguild predator-prey system depend on initial conditions. Journal of
694 Animal Ecology 77:624-630.
695 Morel, F. M. M. 1987. Kinetics of nutrient uptake and growth in phytoplankton. Journal of
696 Phycology 23:137-150.
697 Morin, P. 1999. Productivity, intraguild predation, and population dynamics in experimental food
698 webs. Ecology 80:752-760.
699 Mylius, S. D., K. Klumpers, A. M. De Roos, and L. Persson. 2001. Impact of intraguild predation
700 and stage structure on simple communities along a productivity gradient. American
701 Naturalist 158:259-276.
702 Paerl, H. W., and J. Huisman. 2008. Blooms like it hot. Science 320:57-58.
703 Passarge, J., S. Hol, M. Escher, and J. Huisman. 2006. Competition for nutrients and light: stable
704 coexistence, alternative stable states, or competitive exclusion? Ecological Monographs
705 76:57-72.
706 Polis, G. A., and R. D. Holt. 1992. Intraguild predation: the dynamics of complex trophic
707 interactions. Trends in Ecology and Evolution 7:151-154.
708 Polis, G. A., and D. R. Strong. 1996. Food web complexity and community dynamics. American
709 Naturalist 147:813-846.
710 Polis, G. A., C. A. Myers, and R. D. Holt. 1989. The ecology and evolution of intraguild
711 predation: potential competitors that eat each other. Annual Review of Ecology and
712 Systematics 20:297-330.

713 Qin, B., G. Zhu, G. Gao, Y. Zhang, W. Li, H. W. Paerl, and W. W. Carmichael. 2010. A drinking
714 water crisis in Lake Taihu, China: linkage to climatic variability and lake management.
715 Environmental Management 45:105-112.
716 Raven, J. A. 1997. Phagotrophy in phototrophs. Limnology and Oceanography 42:198-205.
717 Reboud, X., and G. Bell. 1997. Experimental evolution in *Chlamydomona*s. III. Evolution of
718 specialist and generalist types in environments that vary in space and time. Heredity
719 78:507-514.
720 Rosenheim, J. A., H. K. Kaya, L. E. Ehler, J. J. Marois, and B. A. Jaffee. 1995. Intraguild
721 predation among biological control agents: theory and evidence. Biological Control
722 5:303-335.
723 Rudolf, V. H. W., and J. Armstrong. 2008. Emergent impacts of cannibalism and size refuges in
724 prey on intraguild predation systems. Oecologia 157:675-686.
725 Sanders, R. W., D. A. Caron, J. M. Davidson, M. R. Dennett, and D. M. Moran. 2001. Nutrient
726 acquisition and population growth of a mixotrophic alga in axenic and bacterized cultures.
727 Microbial Ecology 42:513-523.
728 Scheffer, M. 1998. Ecology of shallow lakes. Chapman and Hall, London, UK.
729 Skalski, G. T. and J. F. Gilliam. 2001. Functional responses with predator interference: viable
730 alternatives to the Holling type II model. Ecology 82: 3083-3092.
731 Skovgaard, A. 1996. Mixotrophy in *Fragilidium subglobosum* (Dinophyceae): growth and
732 grazing responses as functions of light intensity. Marine Ecology Progress Series
733 143:247-253.
734 Smith, H. L., and P. Waltman. 1994. Competition for a single limiting resource in continuous
735 culture: the variable-yield model. SIAM Journal on Applied Mathematics 54:1113-1131.

736 Sterner, R. W., and J. J. Elser. 2002. Ecological stoichiometry: the biology of elements from
737 molecules to the biosphere. Princeton University Press, Princeton, NJ, USA.
738 Stoecker, D. K. 1998. Conceptual models of mixotrophy in planktonic protists and some
739 ecological and evolutionary implications. European Journal of Protistology 34:281-290.
740 Straub, C. S., D. L. Finke, and W. E. Snyder. 2008. Are the conservation of natural enemy
741 biodiversity and biological control compatible goals? Biological Control 45:225-237.
742 Thingstad, T. F., H. Havskum, K. Garde, and B. Riemann. 1996. On the strategy of "eating your
743 competitor": a mathematical analysis of algal mixotrophy. Ecology 77:2108-2118.
744 Tilman, D. 1982. Resource competition and community structure. Princeton University Press,
745 Princeton, NJ, USA.
746 Urbani, P., and R. Ramos-Jiliberto. 2010. Adaptive prey behavior and the dynamics of intraguild
747 predation systems. Ecological Modelling 221:2628-2633.
748 Van de Waal, D. B., J. M. H. Verspagen, M. Lürling, E. Van Donk, P. M. Visser, and J. Huisman.
749 2009. The ecological stoichiometry of toxins produced by harmful cyanobacteria: an
750 experimental test of the carbon-nutrient balance hypothesis. Ecology Letters 12:1326-
751 1335.
752 Van de Wolfshaar, K. E., A. M. de Roos, and L. Persson. 2006. Size-dependent interactions
753 inhibit coexistence in intraguild predation systems with life-history omnivory. American
754 Naturalist 168:62-75.
755 Van Donk, E., S. Cerbin, S. Wilken, N. R. Helmsing, R. Ptacnik, and A. M. Verschoor. 2009.
756 The effect of a mixotrophic chrysophyte on toxic and colony-forming cyanobacteria.
757 Freshwater Biology 54:1843-1855.

758 Van Maanen, R., G. Broufas, M. F. Oveja, M. W. Sabelis, and A. Janssen. 2012. Intraguild
759 predation among plant pests: western flower thrips larvae feed on whitefly crawlers.
760 BioControl 57:533-539.
761 Van Wichelen, J., I. van Gremberghe, P. Vanormelingen, A. E. Debeer, B. Leporcq, D. Menzel,
762 G. A. Codd, J. P. Descy, and W. Vyverman. 2010. Strong effects of amoebae grazing on
763 the biomass and genetic structure of a *Microcystis* bloom (Cyanobacteria). Environmental
764 Microbiology 12:2797-2813.
765 Verdy, A., and P. Amarasekare. 2010. Alternative stable states in communities with intraguild
766 predation. Journal of Theoretical Biology 262:116-128.
767 Verschoor, A. M., M. Vos, and I. van der Stap. 2004. Inducible defences prevent strong
768 population fluctuations in bi- and tritrophic food chains. Ecology Letters 7:1143-1148.
769 Verspagen, J. M. H., J. Passarge, K. D. Jöhnk, P. M. Visser, L. Peperzak, P. Boers, H. J.
770 Laanbroek, and J. Huisman. 2006. Water management strategies against toxic *Microcystis*
771 blooms in the Dutch delta. Ecological Applications 16:313-327.
772 Wilken, S., S. Wiezer, J. Huisman, and E. Van Donk. 2010. Microcystins do not provide anti-
773 herbivore defence against mixotrophic flagellates. Aquatic Microbial Ecology 59:207-
774 216.
775 Wilken, S., J. M. H. Verspagen, S. Naus-Wiezer, E. Van Donk, and J. Huisman. 2013a
776 Experimental comparison of predator-prey interactions with and without intraguild
777 predation by manipulation of the nitrogen source. Oikos, Early View,
778 DOI: 10.1111/j.1600-0706.2013.00736.x.
779 Wilken, S., J. Huisman, S. Naus-Wiezer, and E. Van Donk. 2013b. Mixotrophic organisms
780 become more heterotrophic with rising temperature. Ecology Letters 16:225-233.

781 Xu, H., H. W. Paerl, B. Qin, G. Zhu, and G. Guo. 2010. Nitrogen and phosphorus inputs control
782 phytoplankton growth in eutrophic Lake Taihu, China. Limnology and Oceanography
783 55:420-432.
784 Yang, Z., and F. Kong. 2012. Formation of large colonies: a defense mechanism of *Microcystis*
785 *aeruginosa* under continuous grazing pressure by flagellate *Ochromonas* sp. Journal of
786 Limnology 71:61-66.
787 Yoshida, T., L. E. Jones, S. P. Ellner, G. F. Fussmann, and N. G. Hairston. 2003. Rapid evolution
788 drives ecological dynamics in a predator-prey system. Nature 424:303-306.
789 Zubkov, M. V., and G. A. Tarran. 2008. High bacterivory by the smallest phytoplankton in the
790 North Atlantic Ocean. Nature 455:224-226.
791
792
793 SUPPLEMENTAL MATERIAL
794 Appendix A
795 Detailed methods of additional experiments to explain the lack of biological control at high
796 nitrogen loads

797 Table 1: Definition and values of model parameters

Symbol	Definition	Value		Unit	Source
State variables					
N	Dissolved inorganic nitrogen concentration			mol/L	
Q_A	Cellular nitrogen content of the autotroph			mol/cell	
Q_M	Cellular nitrogen content of the mixotroph			mol/cell	
A	Population density of the autotroph			cells/L	
M	Population density of the mixotroph			cells/L	
System parameters					
D	Dilution rate	0.12		day^{-1}	a
N_{in}	Nitrogen load	$10^{-8} – 10^{-2}$		mol/L	a
Species parameters		*Microcystis*	*Ochromonas*		
$u_{max,i}$	Maximum N-uptake rate	12.0×10^{-14}	24.0×10^{-14}	mol $cell^{-1}$ day^{-1}	e
K_i	Half-saturation constant	9.0×10^{-7}	6.5×10^{-7}	mol/L	e
$\mu_{max,i}$	Maximum specific growth rate	0.70	2.2	day^{-1}	b

$Q_{min,i}$	Minimum cellular nitrogen content	2.6×10^{-14}	1.0×10^{-13}	mol/cell	c
$Q_{max,i}$	Maximum cellular nitrogen content	9.5×10^{-14}	32×10^{-13}	mol/cell	b,e
f_{max}	Maximum prey ingestion rate	n.a.	53.0	cells cell^{-1} day^{-1}	d
k_M	Half-saturation constant for prey ingestion	n.a.	4.0×10^{8}	cells/L	f
b	Curvature of type III functional response	n.a.	2.37	-	d

a: measured system parameter; b: measured in an independent chemostat experiment with saturating nitrogen concentrations; c: measured after nitrogen starvation in batch culture; d: measured in the grazing experiment of Wilken et al. (2010); e: estimated from earlier monoculture chemostats (Wilken et al. 2013a); f: tuning parameter estimated from model fits to the species mixtures.

801 Figure legends

802

803 Figure 1: Model predictions of the steady-state abundances of the autotroph and
804 mixotroph and the dissolved inorganic nitrogen concentration as function of the nutrient
805 load. Parameter values are provided in Table 1.

806

807 Figure 2: Monoculture experiments of *Ochromonas* (left panels) and *Microcystis* (right
808 panels). The experiments were performed at (A,B) low nitrogen load of 20 μM
809 ammonium, (C,D) intermediate nitrogen load of 100 μM ammonium, and (E,F) high
810 nitrogen load of 500 μM ammonium. Open circles = *Ochromonas*, closed circles =
811 *Microcystis*, open triangles = ammonium concentration.

812

813 Figure 3: Steady-state characteristics of the monocultures plotted as function of the
814 nitrogen load. (A) Steady-state abundances of *Ochromonas* (open circles) and
815 *Microcystis* (closed circles) in the monoculture experiments. (B) Molar C:N ratios of the
816 cells (diamonds) and depth-averaged light intensity (I_{avg}; squares) in the monocultures.
817 (C) Concentration of dissolved ammonium (R^*; triangles) in the monocultures. Open
818 symbols indicate *Ochromonas*, while closed symbols indicate *Microcystis*. Error bars
819 indicate standard errors of repeated measurements during steady state (n=12).

820

821 Figure 4: Intraguild predation experiments. In the left panels, a small amount of
822 *Microcystis* was inoculated in monocultures of *Ochromonas*. In the right panels, a small
823 amount of *Ochromonas* was inoculated in monocultures of *Microcystis*. The experiments

were performed at (A,B) low nitrogen load of 20 μM ammonium, (C,D) intermediate nitrogen load of 100 μM ammonium, and (E,F) high nitrogen load of 500 μM ammonium. Open circles = *Ochromonas*, closed circles = *Microcystis*, open triangles = ammonium concentration. For comparison, horizontal lines give the steady-state abundances of *Ochromonas* (grey lines) and *Microcystis* (black lines) in monoculture. The vertical dotted lines in panels E and F indicate the time point at which the incident light intensity was increased.

Figure 5: Steady-state characteristics of the intraguild predation experiments plotted as function of the nitrogen load. (A) Steady-state abundances of *Ochromonas* (open circles) and *Microcystis* (closed circles) in the intraguild predation experiments. The open triangles show the steady-state concentration of dissolved ammonium. (B) The abundances of *Ochromonas* and *Microcystis* in the intraguild predation experiments relative to their abundances in monoculture. (C) Depth-averaged light intensity (I_{avg}) and molar C/N ratio of the species mixture in the intraguild predation experiment. (D) Steady-state dissolved ammonium concentrations of the *Ochromonas* and *Microcystis* monocultures compared to the intraguild predation experiment. The bars show the means (± s.d.) calculated over all three nitrogen loads using 12 replicate measurements per steady-state culture.

Figure 6: DGGE-gels for the ITSa, ITSb, and ITSc regions of *Microcystis* sampled from the experiments performed at high nitrogen load of 500 μM ammonium. The lanes represent the following samples: M = marker; 1 = day 48 of monoculture; 2 = day 9 of

847 mixed culture; 3 = day 24 of mixed culture; 4 = day 78 of mixed culture; 5 = day 165 of
848 mixed culture.
849
850 Figure 7: Differences in nutritional quality of N-amended versus N-starved cells of
851 *Microcystis*. (A) C:N ratios of *Microcystis*. (B) Grazing rates of *Ochromonas* on
852 *Microcystis*. (C) Growth rates of *Ochromonas* on *Microcystis*. Error bars give standard
853 deviations of triplicate measurements.
854
855 Figure 8: Grazing rates of *Ochromonas* on *Microcystis* as function of *Ochromonas*
856 abundance. Error bars give standard deviations of triplicate measurements. Bars with
857 different letters are significantly different (ANOVA after log-transformation of data to
858 improve homogeneity of variance: $F_{3,8}$ =8.03; P<0.01).
859
860 Figure 9: Model predictions of (A) the intraguild predation model without predation
861 interference and (B) when intraspecific interference among the predators is included (Eqn
862 9). The graphs show steady-state abundances of the autotroph *Microcystis* and the
863 mixotroph *Ochromonas* and the dissolved ammonium concentration as function of the
864 nutrient load. Symbols represent experimental measurements, while lines give model
865 predictions. Parameter values are the same as in Fig. 1 (see Table 1). The interference
866 parameter c takes a value of 2.6×10^{-4} L/cell. In some cases, the measurements from the
867 two independent species mixtures were too similar to be visibly distinguishable in the
868 graph.
869

870 **Figure 1:**

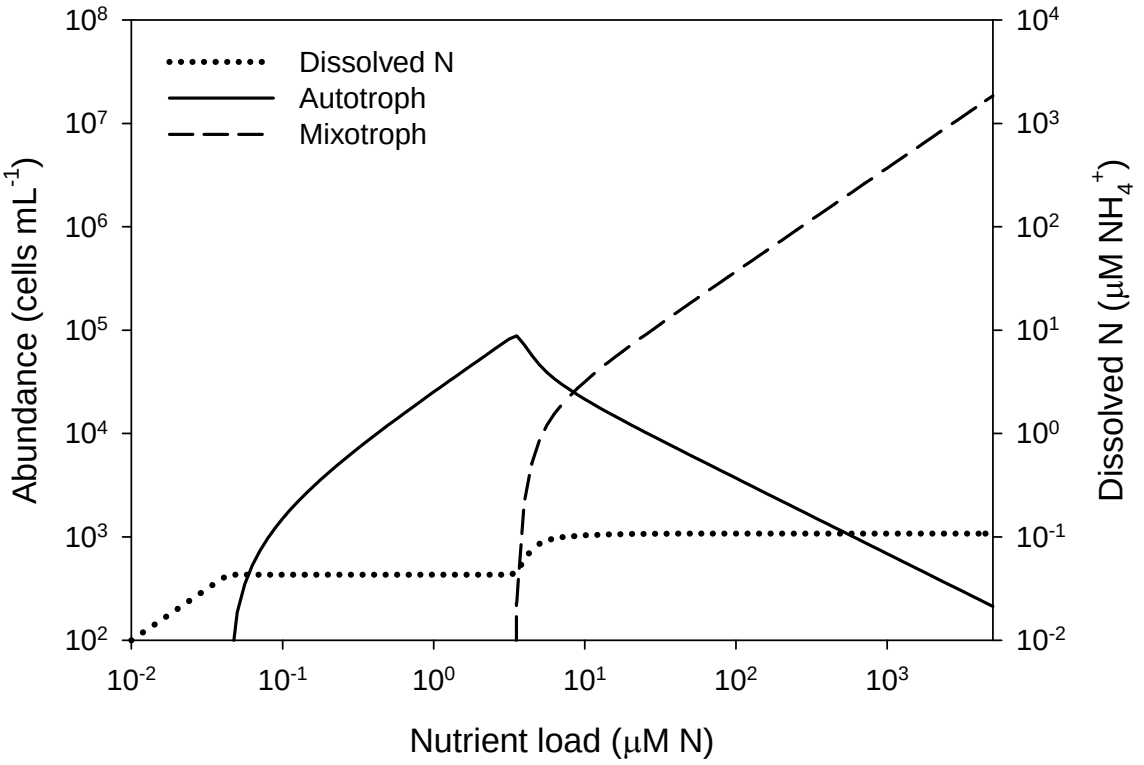

871

872

873 **Figure 2:**

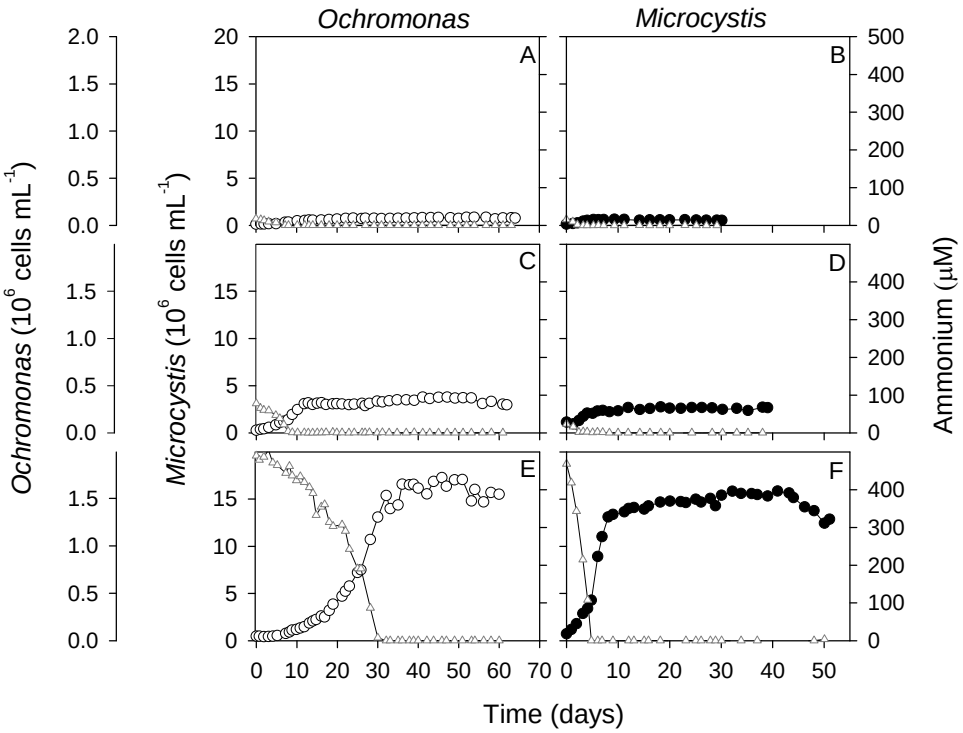

874

875 **Figure 3:**

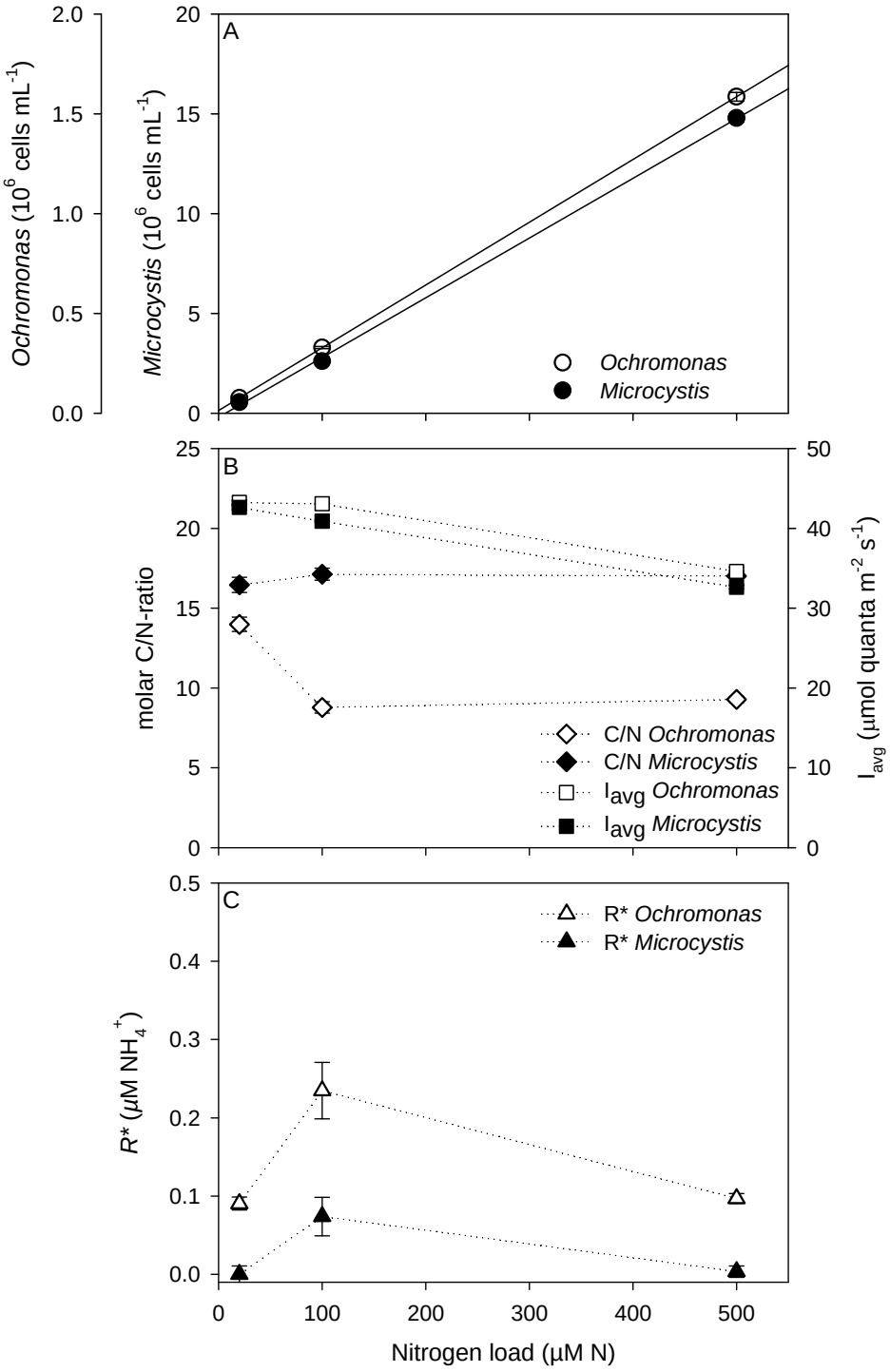

876

877

878 **Figure 4:**

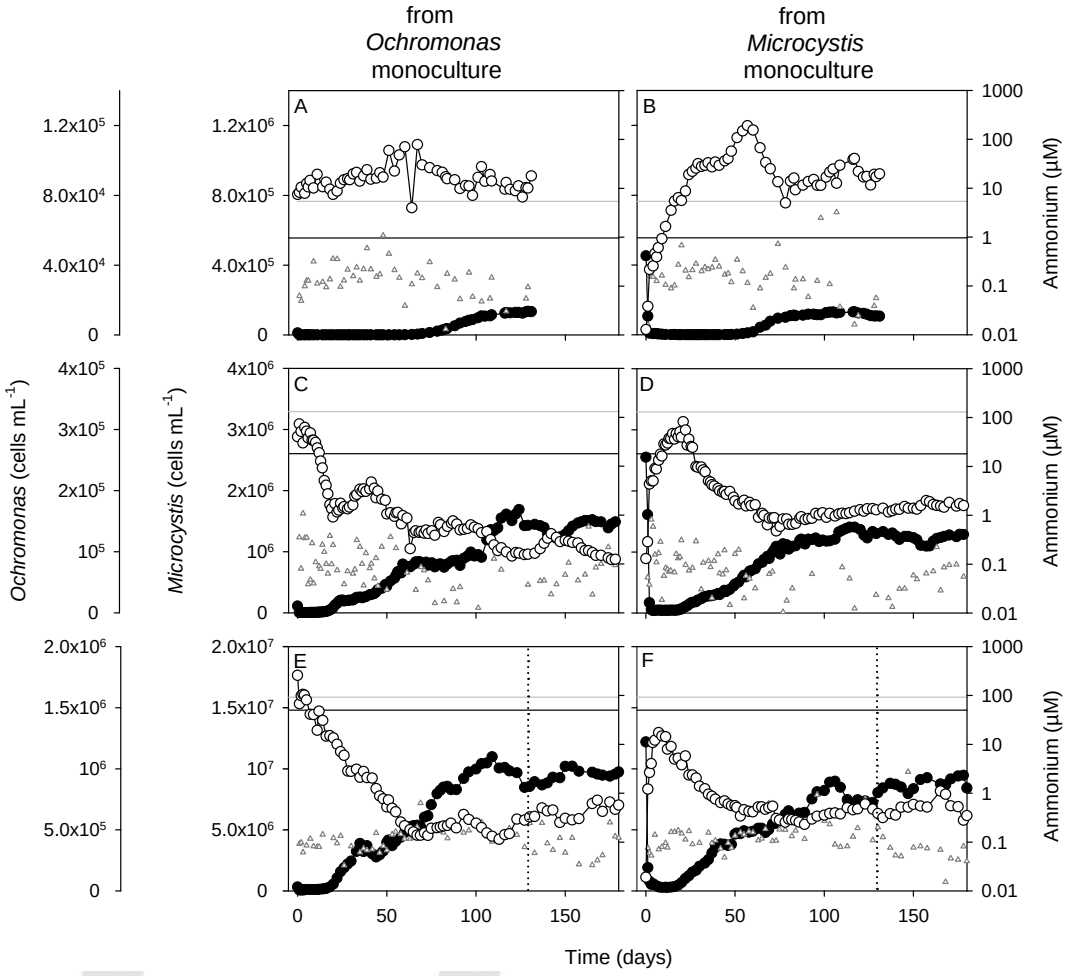

879

880 **Figure 5:**

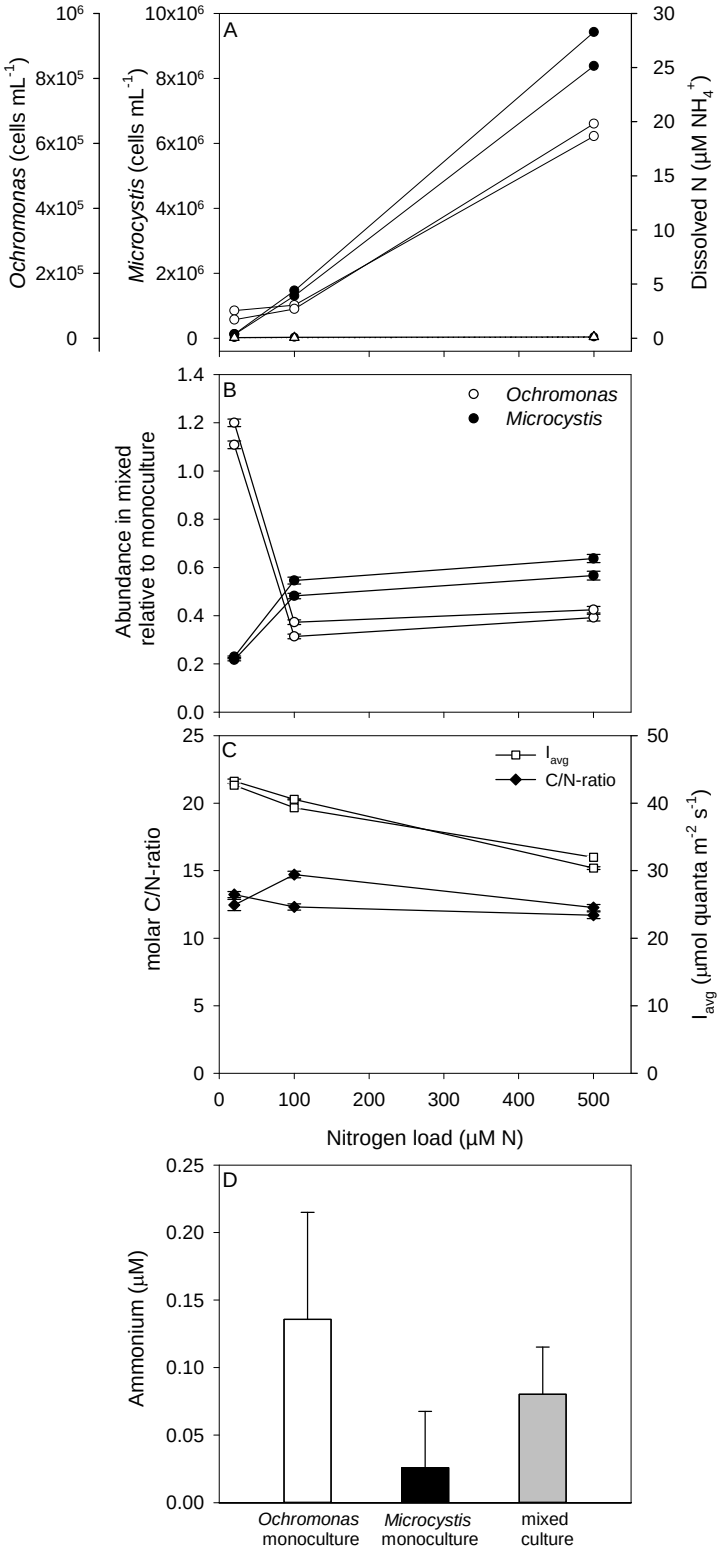

881

882

883 **Figure 6:**

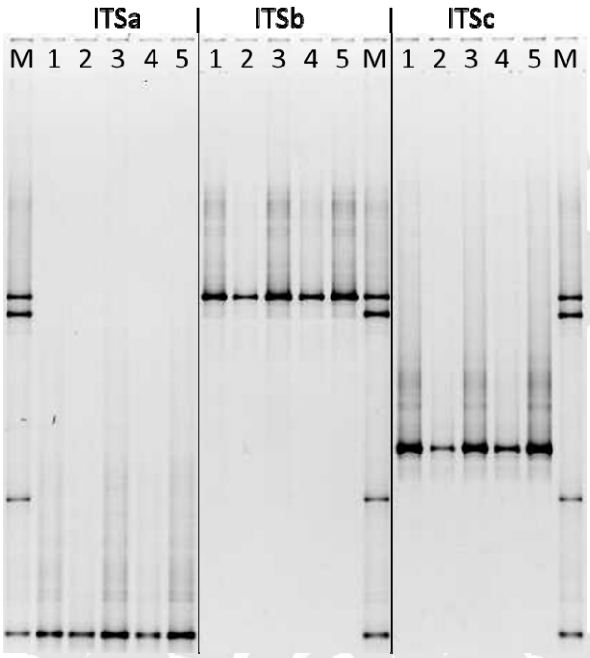

884

885

886 **Figure 7:**

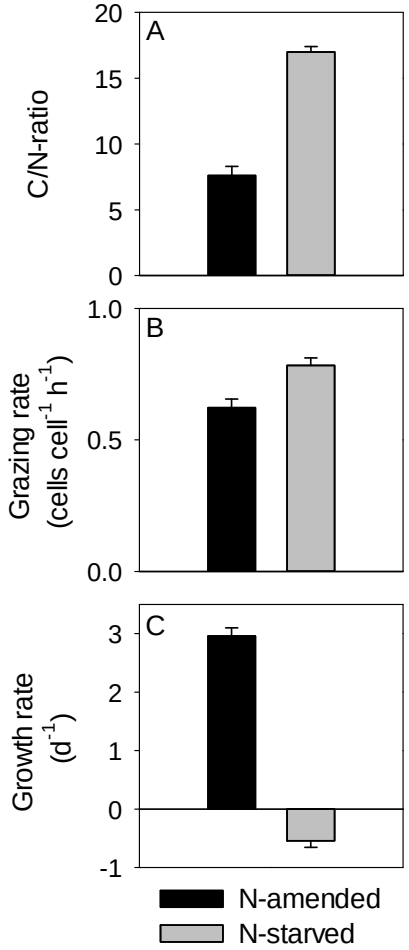

887

888 **Figure 8:**

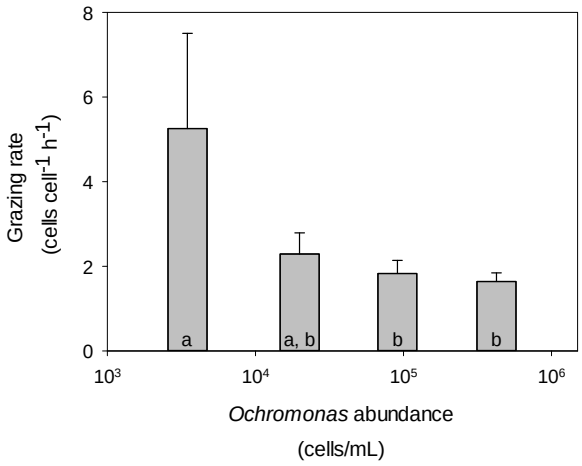

889

890 **Figure 9:**

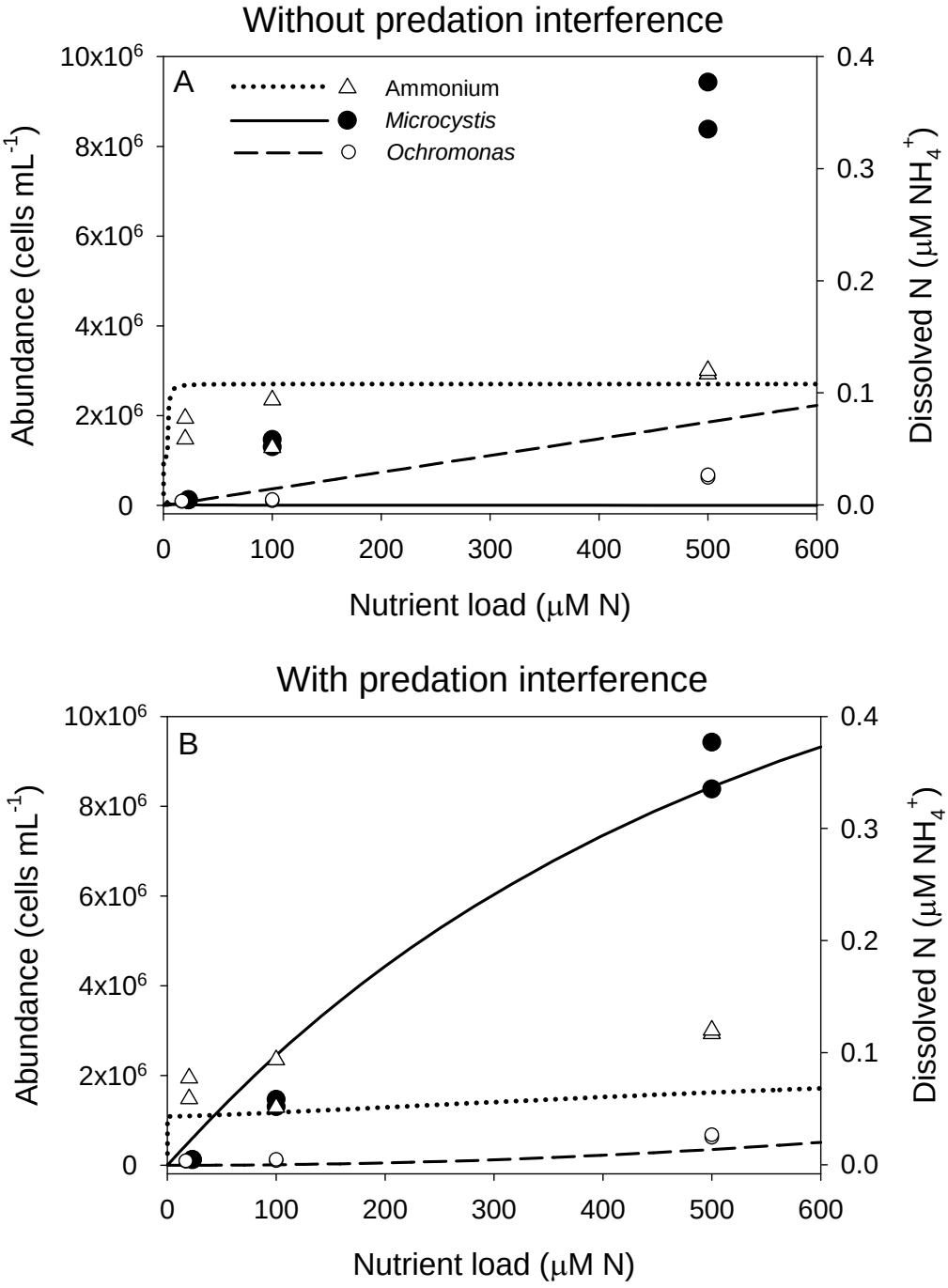

891

892